POTENTIAL FLOW MODELS OF AIRFOILS WITH SEPARATED FLOW

ICAS-86-2.3.3

G.V. Parkinson and W. Yeung
Department of Mechanical Engineering
The University of British Columbia
Vancouver, B.C., Canada

Abstract

In the authors' laboratory there is a long-term program of studying the aerodynamics of airfoils and wings with separated flow through the use of potential flow models. In this paper earlier work is reviewed and new work described. The earlier work includes analytical and numerical thick-airfoil theories for the pressure distribution on airfoils with normal spoilers, using wake sources to simulate wake effects, a thin-airfoil free-streamline theory for the lift and moment on airfoils with spoilers in steady and unsteady flow, and lifting-line theory, incorporating the thin-airfoil theory, for wings fitted with part-span spoilers. In the new work an improved analytical wake-source model is described in which airfoils with inclined spoilers or split flaps can be treated, and an additional boundary condition reduces the empiricism to the minimum required in such flow models. Predictions from both the earlier and the new models are shown to be in good agreement with wind tunnel data.

I. Introduction

It is still impossible to obtain complete solutions, for Reynolds numbers of engineering interest, to problems of separated flow about bodies. Nevertheless, aerodynamicists need to determine the loadings on airfoils and wings experiencing separated flows caused by stall or by the deployment of control devices such as spoilers or split flaps. For an airfoil in unseparated flow the problem can be solved by a combination of an outer potential flow and an inner boundary layer flow. The potential flow alone gives a fairly good estimate of the airfoil pressure distribution, and the combination, by the use of iterative methods, can lead to an accurate calculation of both pressure and shear stress distributions. For airfoils in separated flow, however, the situation is less satisfactory for two reasons. The first is the inability to deal with the interior of the broad wake, usually turbulent and containing organized vortex systems. The second is the uncertainty about wake boundary conditions even if the interior is ignored.

However, since the wake total head is greatly reduced, the airfoil surface exposed to the wake experiences very small shear stresses and a nearly constant time-averaged pressure distribution. This suggests that a potential flow model could give a satisfactory prediction of pressure loading on a body if the pressure were given correctly at the separation points. Of course, a successful model requires a reasonable simulation of the wake boundary conditions but, since these cannot in any case be precisely defined, 'reasonable' may involve no more than having the streamline simulating the separating shear layer start out in the correct direction with the correct velocity.

In a continuing research program in the Department of Mechanical Engineering at the University of British Columbia the application of such potential flow models to airfoils with spoilers in steady and unsteady flow, and the extension to wings of finite span, have been explored and developed. Two basic models have been employed: a thick-airfoil model in which wake effects are simulated by sources on the airfoil surface, and a thin-airfoil model in which the wake is treated as a constant-pressure cavity. In the following sections these models and the results obtained from them are reviewed, and recent improvements and extensions to the wake source model are described and its predictions are compared with experimental data.

2. Types of Model

2.1 Wake Source Model

2.1.1 Analytical Model. The wake source model for symmetrical bluff bodies (Parkinson and Jandali[1]) and its extension to lifting airfoils with normal spoilers (Jandali and Parkinson[2]) use a conformal mapping method leading to simple flow solutions, since the mapping problem is only for the wetted surface of the body. In this model the contour to be mapped is the wetted surface plus an additional contour in the wake providing a slit or cusp at each flow separation point. The part of the original contour exposed to the wake is ignored unless it already conforms to the above requirement. Thus, a circular cylinder is treated as a circular-arc slit, and for the airfoil the spoiler is already a slit, while the trailing edge, if not already a cusp, is converted to one. The resulting contour is then mapped to a circle by a set of transformations for which the overall derivative of the mapping function has simple zeros at the flow separation points. In the transform plane the flow model consists of uniform flow plus a doublet for the basic circle, two sources on the wake portion of the contour and their image sink at the center, and a vortex at the center for the circulation in lifting configurations. The source and vortex strengths and the source angular positions are five unknowns and four of these are determined by conditions at separation. Two conditions are that the separation points in the physical plane become flow stagnation points in the transform plane, thus ensuring tangential separation of the physical streamlines, since angles are doubled there. The other two conditions are the specification of the velocity at the separation points, given by the base pressure on the body, empirically determined as in all such flow models.

For bluff sections with a continuously curved contour, so that flow separation is boundary-layer controlled, the position of the separation points is also specified empirically in the original model, while for the lifting airfoils the number of unknowns to be solved for is kept at four by arbitrarily locating one of the two wake sources close to the transform stagnation point corresponding to the airfoil trailing edge, investigation having shown the result to be relatively insensitive to this source location.

The basic airfoil model uses a Joukowsky profile of arbitrary thickness and camber, fitted with a normal spoiler of arbitrary size and location. The method is easily adapted to an arbitrary airfoil profile with normal spoiler by inserting a Theodorsen[3] transformation into the mapping sequence, as described by Jandali[4]. Fig. 1 shows a typical result, in which the method is used to calculate the pressure distribution on a 14% Clark Y airfoil fitted with an 8.4% normal spoiler at 70% chord. The angle of attack is 10.2° and the theoretical curve is compared with wind tunnel data. Excellent agreement is seen, except just upstream of the spoiler, where a constant-pressure separation bubble occurs instead of the theoretical stagnation point region.

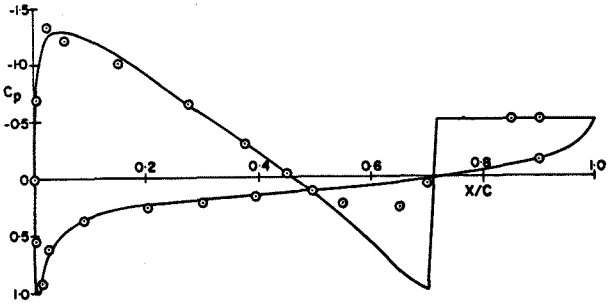

Figure 1. Pressure distribution on 14% Clark Y airfoil with 8.4% normal spoiler at 70% chord. α = 10.2°, ———, theory; o, experiment.

2.1.2 Numerical Model. The conformal mapping method of the previous section is applicable only to single-element airfoils. In order to study the aerodynamics of multi-element airfoils with spoilers, the numerical surface-singularity method of Smith and Hess[5] was adapted to the problem, with the discrete wake sources of the analytical method now used as onset flows, and the same boundary conditions applied. Because of the presence of these finite singularities on the airfoil upper surface it was found necessary to reduce the size of the distributed source elements on the underside of the airfoil opposite them. For an airfoil with spoiler and slotted flap 100 elements on the main foil and 80 on the flap proved satisfactory. Details are given by Brown[6]. Fig. 2 shows two theoretical pressure distributions calculated by the numerical model for a NACA 23012 airfoil at α = 8° with a 25% chord slotted flap deflected 20°. The solid curve is for the airfoil without spoiler, and the dashed curve shows the effect of a 10% normal spoiler at 60% chord. The large lift reduction on the main foil caused by the spoiler is evident, as is the smaller lift increase on the flap. (Such an increase is also observed experimentally, although no experiments were carried out on this profile).

2.2 Linearized Models

2.2.1 Steady Flow Model. The thick-airfoil theories of Section 2.1 are mainly for predicting airfoil pressure distributions, but they can of course also be used to predict lift and pitching moment through numerical integration. However, if the interest is primarily in the lift and moment, there are advantages in employing a thin-airfoil theory because of its relative simplicity. Such a

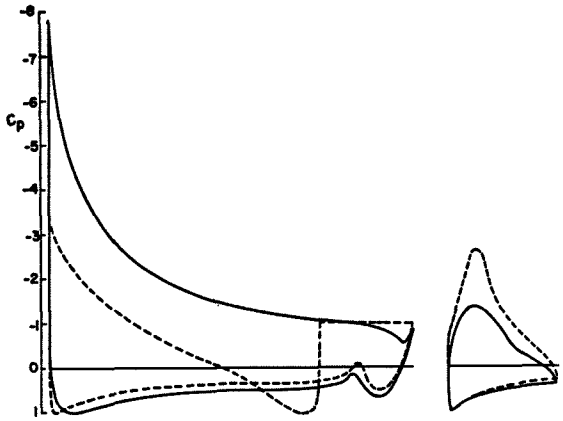

Figure 2. Theoretical pressure distributions on NACA 23012 airfoil at α = 8° with 25% chord slotted flap deflected 20°. ———, basic airfoil; ----- airfoil with 10% normal spoiler at 60% chord.

theory was developed by Brown and Parkinson[7] for a thin airfoil of arbitrary camber and thickness distribution fitted with a spoiler of arbitrary size, location, and deflection angle. In this model the wake is represented by a cavity of finite length with a constant pressure given empirically by the airfoil base pressure coefficient. The linearized airfoil plus cavity is then a finite slit along the real axis in the physical plane, and a sequence of conformal mappings converts the flow field into the upper half of the plane exterior to the unit circle.

In the model the complex acceleration potential is used as the flow variable, and the problem is solved in the transform plane, where the imaginary part of the potential is specified on the unit semi-circle, representing the wetted surface of the airfoil and spoiler, while the real part is specified on the real axis, representing the cavity boundary. The principle of superposition in thin-airfoil theory permits the separate consideration of different aspects of the airfoil geometry, and simple closed-form analytic functions were found for the complex potentials representing effects of angle of attack, and of spoiler deflection either on the basic airfoil or in the presence of a deflected simple flap. On the other hand, series solutions were required for the effects of airfoil camber and thickness. The airfoil lift and pitching moment were calculated using the Blasius integrals. Fig. 3 shows the variation of lift coefficient with angle of attack for a 14% Clark Y airfoil fitted with a 10% spoiler deflected 60° at 70% chord. The straight-line variation predicted by the theory is seen to give good agreement with wind tunnel data.

2.2.2 Unsteady Flow Model. A particular advantage of the acceleration potential as flow variable is its adaptability to unsteady flow problems, and a primary purpose of the work reported in Ref. 7 was to investigate the aerodynamics of transient and oscillatory spoiler motions. The basic model described in Section 2.2.1 was used, with the addition of the appropriate time-dependent velocity and acceleration boundary conditions on the spoiler, and the simplifying approximation of free-stream cavity pressure.

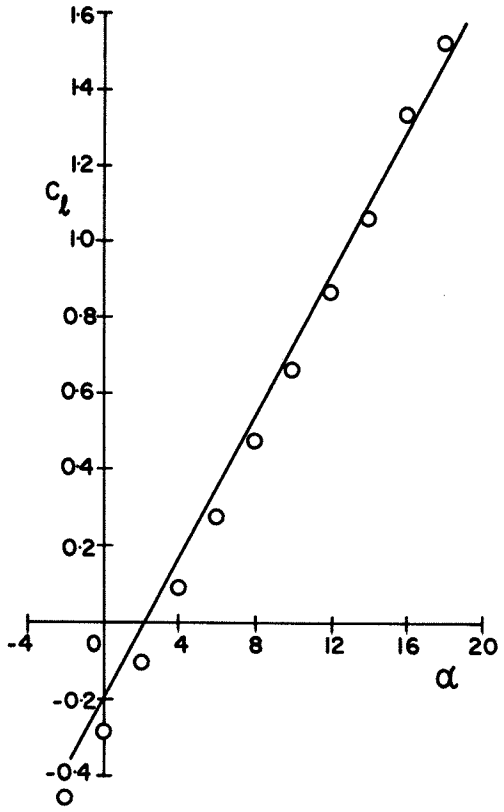

Figure 3. Lift coefficient vs angle of attack for 14% Clark Y airfoil with 10% spoiler deflected 60° at 70% chord. ———, theory; o, experiment.

Solutions were obtained for the transient lift decrement following spoiler activation, and the work was later extended by Bernier and Parkinson[8] to the calculation of transient moment decrement and of spoiler stability derivatives.

In Fig. 4 the transient lift decrement function W is shown as a function of the airfoil travel in chords s' following spoiler activation at a constant erection rate. W is the ratio of the instantaneous lift decrement to the final steady-state decrement, and the theoretical curves are presented for different values of the erection time expressed in chords travel. The calculations are

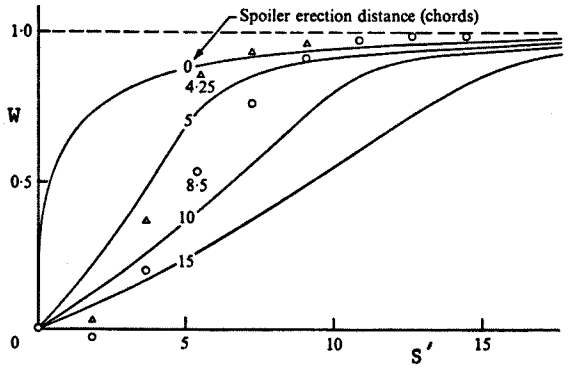

Figure 4. Transient lift decrement function for constant-rate erection of spoiler at 70% chord. ———, theory for 10% spoiler; o, Δ, experiments for 8.4% spoiler on 14% Clark Y airfoil.

for a 10% spoiler at 70% chord, and for comparison experimental data are shown for two different erection times of an 8.4% spoiler at 70% chord on a 14% Clark Y airfoil at 12° angle of attack. The agreement is reasonably good although the experimental rise towards the steady state is more abrupt.

2.3 Lifting-Line Model

Low speed aircraft typically have wings of high aspect ratio so that, if the wings have spoilers or split flaps, it is possible to base a theory for the prediction of the effects of these control surfaces on Prandtl's lifting-line theory[9]. This has been done for wings with spoilers by Tam Doo[10] in a model in which the required airfoil section inputs to lifting-line theory of lift curve slope and zero-lift angle are supplied by thin-airfoil theory. For the portions of the wing span fitted with spoilers the required sectional values are given by the theory of section 2.2.1. The theory gives predictions of wing lift, induced drag, rolling moment, yawing moment, and their spanwise distributions.

Fig. 5 shows the half-wing rolling moment coefficient as a function of angle of attack for a rectangular plan form with full-wing aspect ratio of 7.7. The airfoil section is NACA 0015 and a 10% spoiler deflected 90° at 48% chord occupies 20% of the half wing, with the inboard tip at mid span. The theoretical straight line is compared with data from wind tunnel tests on a half wing, and good agreement is seen.

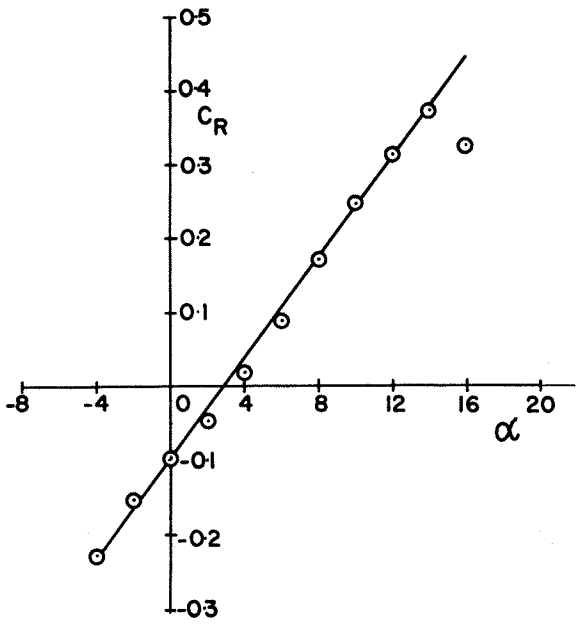

Figure 5. Rolling moment coefficient vs angle of attack for half rectangular wing of aspect ratio 7.7 and NACA 0015 airfoil section fitted with a part-span normal spoiler. ———, theory; o, experiment.

3. Improved Wake Source Model

3.1 Conformal Mappings

Two shortcomings of the original wake source model described in section 2.1.1 were its restriction to airfoils with normal spoilers and its lack of a fifth boundary condition for the five unknown

source and vortex parameters, so that the second source had to be placed arbitrarily close to the airfoil trailing edge. Recent work on the problem has led to the elimination of these shortcomings.

In this section a new sequence of conformal transformations is described by which the field outside an airfoil of Joukowsky profile with an upper-surface spoiler of arbitrary size, inclination to the surface, and chordwise location is mapped into the field outside the unit circle. The sequence, omitting translations, rotations, and scalings, is shown in Figure 6. Minor modifications to this sequence are required to accommodate the configurations of Joukowsky airfoils with lower-surface split flaps. The modification to accommodate a single-element airfoil of arbitrary profile is mentioned later in this section.

The key configuration in the mapping sequence is shown in one of the intermediate transform planes, the s-plane of Figure 6, a circle with a flat fence at angle δ to its surface. Proceeding back in the sequence, a translation and rotation to a t-plane (not shown) puts the center of the circle in the second quadrant and the fence in the first quadrant, while the circle passes through $t = 1$. The Joukowsky transformation,

$$z = t + \frac{1}{t} \tag{1}$$

then maps the circle with fence into a thick, cambered Joukowsky airfoil profile with upper-surface spoiler at angle δ to the surface. In the transformation from s to t the translation (and the original choice of the radius R of the circle) determine the camber and thickness of the airfoil profile, the rotation determines the chordwise position of the spoiler, and the length of the fence determines the spoiler size.

Proceeding forward from the s-plane in the sequence of transformations, use is made of the fact that the circle and fence are on coordinate curves in a bipolar coordinate system. The field exterior to the circle and fence can therefore be mapped to the interior of an infinite strip of the ω-plane, with a slit along the imaginary axis, as shown in Figure 6, by the Karman-Trefftz transformation

$$s = iR \sin \delta \cot \frac{\omega}{2} \tag{2}$$

The segments of the circle above and below the real axis in the s-plane map into the right and left boundaries of the infinite strip, and the fence maps into the slit. The point at infinity in the s-plane (and in the physical z-plane) becomes the origin in the ω-plane. The infinite strip with slit can be regarded as the interior of a degenerate polygon, a suitable subject for a Schwarz-Christoffel transformation to the upper half λ-plane, as shown in Figure 6 for the choice of boundary points leading to the transformation equation

$$\omega = -\frac{\pi}{2}(2 - n) + ih - \frac{i}{2}\left[n \ln\left(\frac{\lambda}{n} + 1\right) + (2 - n) \ln\left(\frac{\lambda}{2 - n} - 1\right)\right] \tag{3}$$

where n and h are defined in the ω-plane. The point λ_∞ now represents the point at infinity in the z-plane. By a translation and scaling transformation to the μ-plane (not shown), λ_∞ is mapped onto $\mu = i$.

Finally, a bilinear transformation and a rotation,

$$\zeta = e^{-i\alpha_o}\left(\frac{i + \mu}{i - \mu}\right) \tag{4}$$

map the upper half μ-plane onto the exterior of the unit circle in the ζ-plane, with the point at infinity now preserved in the overall transformation from the z-plane to the ζ-plane. The purpose of the rotation is to orient the flow at infinity in the ζ-plane in the direction of the real axis, as shown in Figure 6. The angle α_o in Eq. (4) is determined by the angle of attack α of the airfoil in the z-plane, and by geometric parameters of the intermediate transformations.

Only the Joukowsky airfoil profile is studied in the remainder of this paper. However, as in the original model, the theory can be applied to any single-element airfoil profile by employing the method of Theodorsen. The transformation sequences for both the Joukowsky profile and the arbitrary profile satisfy the fundamental requirement of the wake source model that the overall derivative $dz/d\zeta$ has simple zeros at the points corresponding to the flow separation points, here the spoiler tip and airfoil trailing edge. In addition, the body profile must have a slit or cusp at the separation points. For the Joukowsky profile, since the spoiler is a slit and the airfoil trailing edge is a cusp, this requirement is satisfied automatically. However, airfoils of arbitrary profile

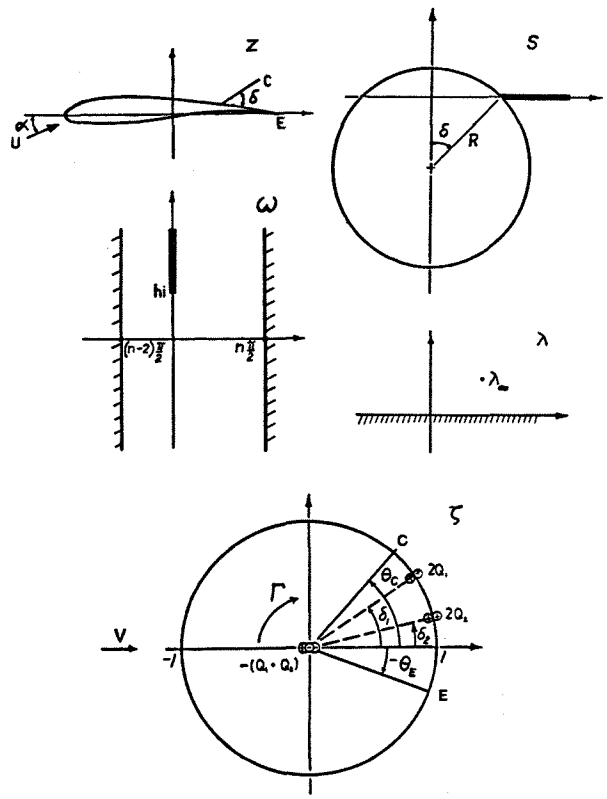

Figure 6. Physical and transform planes for Joukowsky airfoil with spoiler.

generally have finite trailing edge angles. In such cases the upper surface of the airfoil (the part exposed to the wake and therefore not of interest in the flow problem) is modified to make the trailing edge a cusp.

3.2 Flow Model

The flow problem is solved in the ζ-plane, and the equations of this section apply to all airfoil configurations considered in the paper. By the transformations of section 3.1 the problem has been reduced to finding the flow, with uniform velocity V in the direction of the real axis at infinity, past a circular cylinder of unit radius centered at the origin, as shown in Figure 6. There is a circulation about the cylinder and the points corresponding to the two separation points on the airfoil are stagnation points of the cylinder flow. These requirements are satisfied by adding to the familiar basic flow (uniform flow + doublet at origin + vortex of strength Γ at origin) two sources of strengths $2Q_1$, $2Q_2$ on the portion of the cylinder surface downstream of the specified stagnation points. To satisfy the cylinder boundary condition, that its contour is a streamline of the flow, image sinks of strengths Q_1, Q_2 are then added at the origin. This leads to a complex velocity given by

$$w(\zeta) = \frac{dF}{d\zeta} = V\left(1 - \frac{1}{\zeta^2}\right) + \frac{i\Gamma}{2\pi\zeta} + \frac{Q_1}{\pi}\frac{1}{(\zeta - e^{i\delta_1})} + \frac{Q_2}{\pi}\frac{1}{(\zeta - e^{i\delta_2})} - \frac{(Q_1 + Q_2)}{2\pi\zeta} \quad . . . (5)$$

where F is the complex potential, and angles δ_1 and δ_2 are defined in Figure 6. If complex potentials are equated at corresponding points in the ζ- and z-planes, then the contour of the airfoil and spoiler is a streamline of the flow in the z-plane, and its complex velocity is given by

$$w(z) = \frac{w(\zeta)}{dz/d\zeta} \qquad (6)$$

As $z,\zeta \to \infty$, $w(z) \to Ue^{-i\alpha}$ and $w(\zeta) \to V$, which can therefore be determined as a function of U and geometric parameters of the transformations by calculating

$$\left|\frac{dz}{d\zeta}\right|_{z\to\infty}.$$

3.3 Boundary Conditions

The flow model given by Eqs. (5) and (6) automatically satisfies the boundary conditions on w(z) of uniform flow at infinity and tangent flow over the body surface. However, Eq. (5) contains the five unknown parameters Q_1, Q_2, δ_1, δ_2, and Γ, requiring five additional boundary conditions. As mentioned in section 2.1.1, two of these are supplied by the basic requirement that the flow separation points in the z-plane must become flow stagnation points in the ζ-plane (points C and E in both planes in Figure 6).

$$w(\zeta)|_C = w(\zeta)|_E = 0 \qquad (7)$$

Then, since C and E are critical points of the overall transformation, angles are doubled there in the z-plane and the separating streamlines leave the airfoil surface tangentially at the spoiler tip and airfoil trailing edge. Two more boundary conditions are supplied though the empirical assumption of a constant base pressure coefficient C_{pb} over the portion of the airfoil and spoiler surface exposed to the wake in the real flow. In the flow model this leads to the specification of the separation velocity at C and E in the z-plane, through Bernoulli's equation:

$$\left|\frac{w(z)}{U}\right|_C = \left|\frac{w(z)}{U}\right|_E = \sqrt{1 - C_{pb}} \qquad (8)$$

In the mathematical model the flow in the wake region inside the separating streamlines, which simulate the shear layers of the real flow, is of no interest and is ignored, except for its influence on the outer flow as discussed later. The use of L'Hôpital's rule for indeterminate forms is needed to evaluate the boundary conditions given by Eq. (8), since both $w(\zeta)$ and $dz/d\zeta$ in Eq. (6) are zero at points C and E.

Thus, four of the unknown parameters are determined by Eqs. (7) and (8) and in the original version of the airfoil model these were chosen to be Q_1, Q_2, δ_1, and Γ, while the fifth unknown δ_2 was dealt with by empirically placing the source close to E in the ζ-plane, as mentioned in section 1. This gives satisfactory results, since $Q_2 \to 0$ as the source approaches E, and so the aerodynamic loading on the airfoil is relatively insensitive to the exact value of δ_2. However, the additional empiricism is undesirable, and so for the new version of the model an effort was made to devise a fifth boundary condition with a reasonable physical basis. It should be mentioned that one alternative suggestion was to regard the vortex as an unnecessary addition to the flow model and thus eliminate Γ, leaving only four unknowns to satisfy the four boundary conditions, as in the original wake source model for non-lifting bodies. However, this failed completely to produce realistic results for airfoils with spoilers or split flaps.

Therefore, Γ is needed to determine the airfoil circulation, and it is reasonable to assume that the fifth boundary condition should be related to the circulation. In the real flow, the wake region makes no contribution to the time-averaged airfoil circulation, which is therefore a consequence of the unseparated flow upstream of the spoiler tip and airfoil trailing edge. If, then, in the flow model the wake region is also required to make no contribution to the airfoil circulation, the upstream flow should be a better simulation of the real flow. Thus, a suitable fifth boundary condition is

$$\Gamma_w = \mathrm{Re}\int_w w(z)dz = \mathrm{Re}\int_w w(\zeta)d\zeta = 0 \qquad (9)$$

where the integral is over the portion of the contour exposed to the wake in the z-plane or, more usefully, in the ζ-plane, since the integral is preserved in the transformation. The combination of Eqs. (7), (8), and (9) gives five equations for the five unknown constants, and gives good results for airfoils with spoilers (these remarks also apply to split flaps) located relatively near the airfoil trailing edge and with $\delta < 45°$. However, if the spoiler is too far forward or if δ is too large, the equations cannot be satisfied unless the empirical value of C_{pb} is adjusted. This can still lead to a satisfactory simulation of the airfoil pressure distribution except near the separation points, but it would of course be desirable to use the true experimental value of C_{pb}, rather than an

adjusted value, in all cases. The second author has proposed a procedure which achieves this objective as follows.

In Ref. 2, in addition to the version of the flow model described earlier in this section, a simpler version called the one-source model was also presented. In it one source is eliminated, so that $Q_2 = \delta_2 = 0$ and only the three unknowns Q_1, δ_1, Γ remain to be determined by the two equations (7) and one of (8). In this way tangential flow at separation is achieved, but at the correct velocity at only one of the separation points, so that there is in general a pressure discontinuity at the other one. However, the simulation of the complete airfoil pressure distribution is quite good, and if the one-source model equations are solved twice for a given airfoil-spoiler configuration, with Eq. (8) satisfied first at the spoiler tip and then at the airfoil trailing edge, the two theoretical curves of pressure distribution typically bracket the experimental points closely. In the proposed procedure the integral Γ_w of Eq. (9) is evaluated with the integral $w(\zeta)$ supplied by a solution of the one-source model. Instead of zero, values Γ_{w1} and Γ_{w2} are obtained from the two possible one-source solutions for a given airfoil-spoiler configuration. Then, for the fifth boundary condition in the original problem of the two-source model, Eq. (9) is replaced by

$$\Gamma_w = \mathrm{Re} \int_w w(\zeta)d\zeta = \frac{1}{2} (\Gamma_{w1} + \Gamma_{w2}) \qquad (10)$$

In Eq. (10), the right side is not necessarily zero, but in view of the behaviour of the one-source model solutions it is expected that this boundary condition will ensure a flow outside the wake region that closely simulates the real flow. The procedure is akin to an iterative method. In test applications to airfoil-spoiler and airfoil-split flap configurations, it has always proved possible to satisfy the set of five boundary conditions given by Eqs (7), (8), and (10) with only the experimental value of C_{pb} as an empirical input, so as a result this procedure has been adopted as standard. The result of course is not the solution of a complete boundary value problem because the conditions along the free streamlines bounding the wake region are undefined in wake source models except at separation and at infinity.

3.4 Method of Solution

The simultaneous solution of the five equations (7), (8), and either (9) or (10) for the five unknown parameters Γ, Q_1, Q_2, δ_1, and δ_2 is complicated by the fact that in all of the equations, while Γ, Q_1, and Q_2 enter linearly, angles δ_1 and δ_2 enter nonlinearly, so that a numerical solution is required. Of several procedures tried, the following has been found the most satisfactory.

Since for an acceptable solution the sources must be located on the part of the contour exposed to the wake, in Figure 6

$$\theta_E < \delta_1, \delta_2 < \theta_C$$

where $\zeta = e^{i\theta}$ on the circle in the ζ-plane. Therefore, δ_2 is assigned one of a set of values

$$\delta_2 = \theta_E + \frac{(\theta_C - \theta_E)m}{n+1}, \quad m = 1,2,\ldots,n \qquad (11)$$

and Eqs (7) and (8) are used to solve for the remaining unknowns Γ, Q_1, Q_2, δ_1. This is done by successively eliminating the linear parameters Γ, Q_1, Q_2, and solving the remaining relation numerically for δ_1. Γ, Q_1, and Q_2 are next obtained by substitution. These tentative solutions are then substituted in either Eq. (9) or (10), and will not in general satisfy the equation, so that a residue is left. If so, the next value of δ_2 is assigned from the sequence given by Eq. (11) and the entire procedure is repeated until the residue is found to vanish or change sign, thus assuring a solution. With the parameters determined, $w(\zeta)$ is given by Eq. (5), $w(z)$ by Eq. (6), and the airfoil pressure distribution by Bernoulli's equation

$$C_p = 1 - \left| \frac{w(z)}{U} \right|^2 \qquad (12)$$

3.5 Experiments

Experiments were performed for two purposes, first, to measure the base pressure values that form the required empirical input to the theory, second, to make comparisons between the theoretical and experimental pressure distributions on the airfoil at different angles of attack and for the various configurations involved.

Two series of experiments were carried out: one involving the airfoil and spoilers, and the other with the airfoil and split flaps. They were conducted in the laboratory's small low speed aeronautical wind tunnel, in which all of the previous experimental results of Section 2 had been obtained. It has a test section of 27 in. height and 36 in. width. The tunnel possesses good flow uniformity and a turbulence level of less than 0.1 percent over its speed range. The Joukowsky airfoil of 27 in. span, 12.08 in. chord, 11% thickness and 2.4% camber was mounted vertically, with small clearances at the ceiling and the floor, on a six component pyramidal balance situated beneath the test section of the tunnel.

The airfoil was originally designed for Jandali's experiments on normal upper surface spoilers, described in Ref. 2, and there is a point worth noting. Since the Joukowsky profile was structurally weak near the cusped trailing edge, the upper surface in this portion was thickened to give an approximately constant thickness of 1/8 inch. This modified portion does not influence the pressure measurements for the upper surface spoiler experiments because then it is completely embedded in the wake and has no effect on the outer flow. However, it does lead to some error in pressure measurement near the upper surface trailing edge in airfoil experiments with lower surface split flaps. It would have been preferable for the split flap experiments to have this modified portion located on the lower surface of the airfoil so that it would again be exposed to the wake.

In the experiments, end plates on the airfoil were used to allow the spoiler or split flap to be located at various positions and angles of inclination. The spoilers of height 5% and 10% chord could be mounted at distances of 50%, 70%, and 90% chord from the leading edge of the airfoil. The 5% chord spoiler could only be inclined at 45° whereas that of 10% chord could be deflected at 30° or 60° with respect to the local upper surface of the airfoil. The two split flaps used were of 20% and 30% chord, located at their chord distance from the

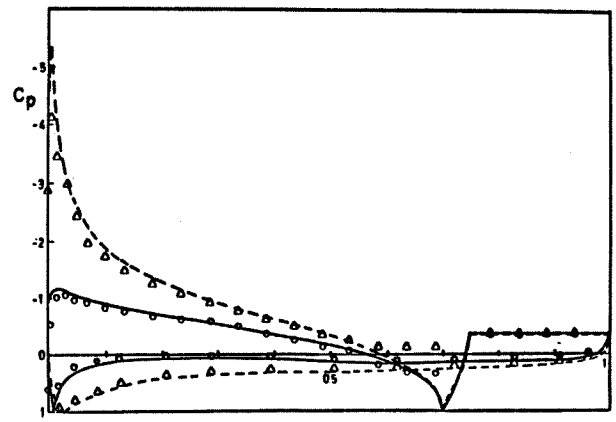

Figure 7. Pressure distributions on Joukowsky airfoil with 5% spoiler at 70% chord. $\delta = 45°$. ———, theory; c, experiment: $\alpha = 6°$. - - - - -, theory; Δ, experiment: $\alpha = 12°$.

trailing edge. The angles of inclination were 10°, 30°, 45°, and 60°. The small gap between the spoiler or flap and the airfoil surface was sealed.

Owing to the small sizes of spoilers used, pressure measurements were made only on the wetted surface of each flap. They were obtained by taping pressure tubing over the surface so that the tubes were exposed to the outer flow. The pressures on the surface of the airfoil, including the portion within the wake, however, were measured by using the pressure taps built into the Joukowsky airfoil. All pressure taps were connected to a 48 port scanivalve, a manually scanning pressure transducer. A Setra 237 differential pressure transducer, a HP 6204B D.C. power supply, a Solartron JM 1860 time domain analyser and a Fluke 8000A digital multimeter were used for data recording.

In addition to supporting the airfoil, the balance was used to measure not only the lift, but the drag and pitching moment, needed for the wind tunnel wall corrections, which were made to the data by standard methods. The test Reynolds number was $3(10)^5$.

3.6 Results

3.6.1 Spoiler. Samples of the theoretical and experimental results obtained for the Joukowsky airfoil fitted with different upper-surface spoilers are given in Figures 7-9. Boundary condition Eq.(10) was used in the theoretical solutions. In Figure 7 pressure distributions are shown for the airfoil with a 5% spoiler at 45° located at 70% chord. Theoretical curves are compared with experimental data for two angles of attack, and good agreement is seen in both cases except just upstream of the spoiler, where in the experiments the adverse boundary layer pressure gradient has produced a constant-pressure separation bubble instead of the potential-flow stagnation-point region. As would be expected, this bubble is larger at $\alpha = 12°$ than at $\alpha = 6°$.

In Figures 8 and 9 pressure distributions are shown for the airfoil with a 10% spoiler located at 70% chord. Comparisons between theoretical and experimental results are given for two spoiler deflections and two angles of attack, and again good agreement is seen except for the presence of the spoiler separation bubbles. Results similar to those of Figures 7-9 were obtained for other spoiler-airfoil configurations tested.

3.6.2 Split Flap. Split flaps, although not now as widely used on aircraft as spoilers, are still important. Several current designs employ them rather than simple flaps or slotted flaps because of their simplicity and combined high lift and drag characteristics, effective in the landing approach. Since, the split flap can be regarded as a spoiler transferred from the airfoil upper surface to the trailing edge portion of the lower surface, no basic changes are required in the theory for the sequence of conformal transformations or for the flow model. There are some minor changes in the transformation equations arising from the geometric differences in the two systems.

Figure 10 shows comparisons of theoretical and experimental pressure distributions for the Joukowsky airfoil at 4° angle of attack with the 20% chord split flap deflected 10°, 30°, and 60°. For all three cases there is close agreement between theory and experiment, with the following exceptions. As in all the experimental data for

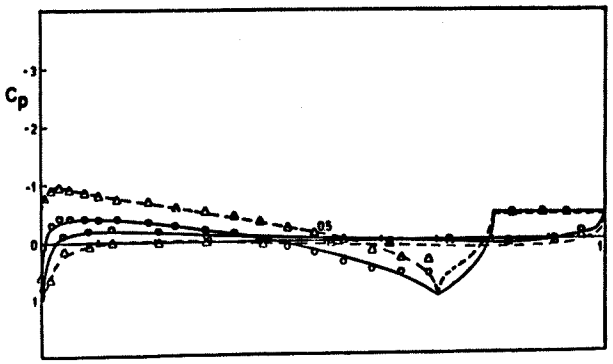

Figure 8. Pressure distributions on Joukowsky airfoil with 10% spoiler at 70% chord. $\alpha = 6°$. - - - - -, theory; Δ, experiment: $\delta = 30°$. ———, theory; o, experiment: $\delta = 60°$.

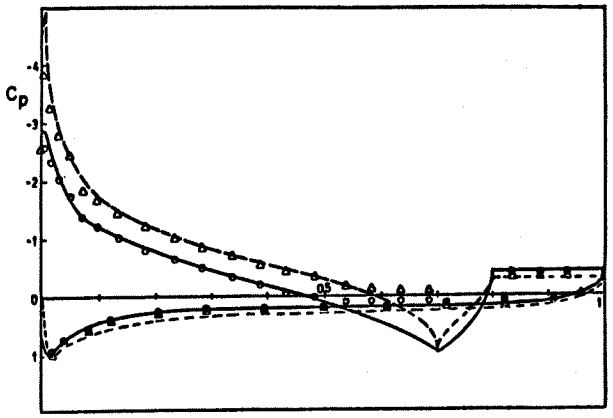

Figure 9. Pressure distributions on Joukowsky airfoil with 10% spoiler at 70% chord. $\alpha = 12°$. - - - - -, theory; Δ, experiment: $\delta = 30°$. ———, theory; o, experiment: $\delta = 60°$.

the Joukowsky airfoil with split flap, the data point nearest the trailing edge for the upper surface should be disregarded, since it reflects the artificial thickening of that portion. For $\delta = 60°$, the theory overestimates the leading-edge suction peak, presumably because of boundary-layer effects in reducing the circulation. For $\delta = 10°$, the theoretical pressure distribution on the upstream surface of the flap is more positive than the experimental distribution. Results similar to those of Fig. 10 were obtained for other split-flap configurations tested.

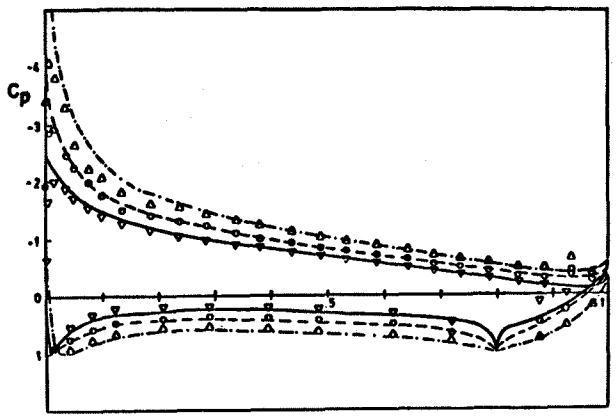

Figure 10. Pressure distributions on Joukowsky airfoil with 20% split flap. $\alpha = 4°$,
———, theory; ∇, experiment: $\delta = 10°$.
– – – –, theory; o, experiment: $\delta = 30°$.
—•—, theory; Δ, experiment: $\delta = 60°$.

4. Discussion

The review of previous work in section 2 indicates considerable success in the use of potential flow models to predict aerodynamic characteristics of airfoils and wings fitted with spoilers. The results in Figs. 7-10 show that the improved wake source model, in addition to having wider applicability with less empiricism, continues to give good predictions of pressure distribution on an airfoil with a spoiler or split flap. The model is convenient to use since the flow system given by Eq. (5) is very simple and the sequence of conformal mappings, while algebraically more complicated than in Refs. 1 or 2, is still relatively easy to deal with in calculations.

The separation bubble in front of the control surface is not modelled, but its neglect appears to produce a purely local discrepancy in the pressure distribution for the airfoil with spoiler, and no significant effect at all for the airfoil with split flap.

The model requires one empirical input, the experimental value of C_{pb}. This is true of all bluff-body potential flow models, and cannot be avoided since C_{pb} is determined mainly by the wake dynamics, which are not modelled. However, two facts diminish the importance of this residual empiricism. First, the experimental variation of C_{pb} is quite small for both spoilers and split flaps, with values generally in the range -0.6 to -0.4 except at very small values of δ. (Here it should be pointed out that the model may not be applicable to some configurations with spoilers at small deflection angles because of possible flow reattachment near the airfoil trailing edge). Second, the theoretical airfoil pressure distribution is relatively insensitive to the value of C_{pb} used. Therefore, given an arbitrary configuration of an airfoil with a spoiler or split flap, one might guess at a C_{pb} of, say, -0.5 and expect the model to give quite a good prediction of the pressure distribution. This improved wake source model could be adapted to the numerical surface singularity method of section 2.1.2 so that multi-element airfoils with spoilers could be treated.

Finally, another possible use of the model is worth mentioning. The sequence of conformal transformations can be modified to provide for tangential streamline separation from any point of the airfoil surface. Using this, perhaps in iterative combination with boundary layer calculations, one could create a model of airfoil stall. Some preliminary work has been done on this problem.

Acknowledgments

The experiments on split flaps were carried out by T.Y. Lu. Financial support for the entire study was provided through a grant from the Natural Sciences and Engineering Research Council of Canada.

References

1. Parkinson, G.V., and Jandali, T., "A Wake Source Model for Bluff Body Potential Flow", Jour. Fluid Mech., 40, 3, 1970, pp. 577-594.

2. Jandali, T., and Parkinson, G.V., "A Potential Flow Theory for Airfoil Spoilers", Trans. C.A.S.I., 3, 1, 1970, pp. 1-7.

3. Theodorsen, T., "Theory of Wing Sections of Arbitrary Shape", NACA TR411, 1931.

4. Jandali, T., "A Potential Flow Theory for Airfoil Spoilers", Ph.D. Thesis, University of British Columbia, 1970.

5. Hess, J.L., and Smith, A.M.O., "Calculation of Potential Flow about Arbitrary Bodies", Prog. in Aero. Sci., 8, Pergamon, 1966.

6. Brown, G.P., "Steady and Nonsteady Potential Flow Methods for Airfoils with Spoilers", Ph.D. Thesis, University of British Columbia, 1971.

7. Brown, G.P., and Parkinson, G.V., "A Linearized Potential Flow Theory for Airfoils with Spoilers", 57, 4, 1973, pp. 695-719.

8. Bernier, R., and Parkinson, G.V., "Oscillatory Aerodynamics and Stability Derivatives for Airfoil Spoiler Motions", Proc. AGARD Conf. on Dynamic Stability Parameters, Athens, 1978, pp. 25-1 to 25-7.

9. Prandtl, L., "Applications of Modern Hydrodynamics to Aeronautics", NACA TR 116, 1921.

10. Parkinson, G.V., and Tam Doo, P., "Prediction of Aerodynamic Effects of Spoilers on Wings", Proc. AGARD Conf. Prediction of Aerodynamic Loading, NASA Ames, 1976, pp. 5-1 to 5-9.